Critical points of quadratic renormalizations of random variables and phase transitions of disordered polymer models on diamond lattices

Cécile Monthus and Thomas Garel
Service de Physique Théorique, CEA/DSM/SPhT, Unité de Recherche Associée au CNRS, 91191 Gif-sur-Yvette Cedex, France
(Received 4 October 2007; published 28 February 2008)

We study the wetting transition and the directed polymer delocalization transition on diamond hierarchical lattices. These two phase transitions with frozen disorder correspond to the critical points of quadratic renormalizations of the partition function. (These exact renormalizations on diamond lattices can also be considered as approximate Migdal-Kadanoff renormalizations for hypercubic lattices.) In terms of the rescaled partition function $z=Z/Z_{\rm typ}$, we find that the critical point corresponds to a fixed point distribution with a power-law tail $P_c(z) \sim \Phi(\ln z)/z^{1+\mu}$ as $z \to +\infty$ [up to some subleading logarithmic correction $\Phi(\ln z)$], so that all moments z^n with $n>\mu$ diverge. For the wetting transition, the first moment diverges $\overline{z}=+\infty$ (case $0<\mu<1$), and the critical temperature is strictly below the annealed temperature $T_c<T_{\rm ann}$. For the directed polymer case, the second moment diverges $\overline{z^2}=+\infty$ (case $1<\mu<2$), and the critical temperature is strictly below the exactly known transition temperature T_2 of the second moment. We then consider the correlation length exponent ν: the linearized renormalization around the fixed point distribution coincides with the transfer matrix describing a directed polymer on the Cayley tree, but the random weights determined by the fixed point distribution $P_c(z)$ are broadly distributed. This induces some changes in the traveling wave solutions with respect to the usual case of more narrow distributions.

DOI: 10.1103/PhysRevE.77.021132 PACS number(s): 02.50.−r, 05.10.Cc, 75.10.Nr

I. INTRODUCTION

A. Real-space renormalizations for disordered systems

The choice to work in real space to define renormalization procedures, which is already interesting for pure systems [1], becomes the unique choice for disordered systems if one wishes to describe spatial heterogeneities. Whenever these disorder heterogeneities play a dominant role over thermal or quantum fluctuations, the most appropriate renormalizations are strong disorder renormalizations [2] introduced by Ma-Dasgupta [3]: as shown by Fisher [4], these strong disorder renormalization rules lead to asymptotic exact results if the broadness of the disorder distribution grows indefinitely at large scales. However, for disordered systems governed by finite-disorder fixed points, where disorder fluctuations remain of the same order of thermal fluctuations, one needs to use more standard real-space renormalization procedures, such as Migdal-Kadanoff block renormalizations [5]. They can be considered in two ways, either as approximate renormalization procedures on hypercubic lattices, or as exact renormalization procedures on certain hierarchical lattices [6,7]. One of the most studied hierarchical lattice is the diamond lattice which is constructed recursively from a single link called here generation $n=0$ (see Fig. 1): Generation $n=1$ consists of b branches, each branch containing two bonds in series; generation $n=2$ is obtained by applying the same transformation to each bond of the generation $n=1$. At generation n, the length L_n between the two extreme sites A and B is $L_n=2^n$, the total number B_n of bonds is $B_n=(2b)^n=L_n^{d_{\rm eff}}$ so that $d_{\rm eff}(b)=\frac{\ln(2b)}{\ln 2}$ represents some effective dimensionality.

On this diamond lattice, various disordered spin models have been studied, such as, for instance, the diluted Ising model [8], random bond Potts model [9], and spin glasses [10]. Disordered polymer models have also been considered, in particular, the wetting on a disordered substrate [11,12] and the directed polymer model [13–21]. In this paper, we focus on these two polymer models that are described by quadratic renormalization of their partition functions as we now recall.

B. Wetting transition with disorder on the diamond lattice

On the diamond lattice, the adsorption of a polymer on a disordered substrate is described by the following quadratic recursion for the partition function Z_n of generation n [11]:

$$Z_{n+1} = Z_n^{(1)} Z_n^{(2)} + (b-1) Y_n^2, \tag{1}$$

where $Y_n=b^{L_n-1}$ represents the number of walks between the two extreme points and satisfies the recursion without disorder

$$Y_{n+1} = b Y_n^2 \tag{2}$$

and where $Z_n^{(1)}$ and $Z_n^{(2)}$ represent two independent copies of generation n. At generation $n=0$, the lattice reduces to a

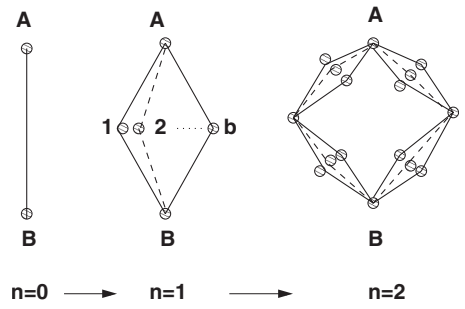

FIG. 1. Hierarchical construction of the diamond lattice of branching ratio b.

single bond with a random energy ϵ, for instance, drawn from the Gaussian distribution

$$\rho(\epsilon) = \frac{1}{\sqrt{2\pi}} e^{-\epsilon^2/2} \tag{3}$$

and thus the initial condition for the recursion of Eq. (1) is simply

$$Z_{n=0} = e^{-\beta\epsilon}. \tag{4}$$

The temperature only appears in this initial condition.

C. Directed polymer on the diamond lattice

The model of a directed polymer in a random medium [22] can also be studied on the diamond hierarchical lattice [13–21]. The partition function Z_n of the n generation satisfies the exact recursion [14]

$$Z_{n+1} = \sum_{a=1}^{b} Z_n^{(2a-1)} Z_n^{(2a)}, \tag{5}$$

where $(Z_n^{(1)}, \ldots, Z_n^{(2b)})$ are $(2b)$ independent partition functions of generation n. At generation $n=0$, the lattice reduces to a single bond with a random energy ϵ, for instance, drawn from the Gaussian of Eq. (3) and thus the initial condition for the recursion of Eq. (5) is again given by Eq. (4).

D. Organization of the paper

In this paper, we study the critical points of the quadratic renormalizations described above that correspond to delocalization transitions for the polymer. These two transitions are of course different in nature, since the wetting transition already exists in the pure case, whereas the directed polymer transition only exists in the presence of disorder. However, we will show below that the quadratic form of the renormalizations induce some common properties. It is thus interesting to study them along the same lines to stress their similarities and differences. The paper is organized as follows. The wetting transition on a disordered substrate is discussed in Sec. II, and studied numerically in Sec. III. The directed polymer transition is discussed in Sec. IV, and studied numerically in Sec. V. In Sec. VI, we compare the results on the diamond lattice with respect to the same disordered polymer models defined on hypercubic lattices. Section VII contains the conclusion. The Appendix contains a reminder on multiplicative stochastic processes which is used in Secs. II and IV.

II. WETTING ON A DISORDERED SUBSTRATE

To study the wetting recursion, it is convenient to introduce the reduced partition function z_n and the associated free-energy f_n defined by [11]

$$z_n \equiv \frac{Z_n}{Y_n} \equiv e^{-\beta f_n} \tag{6}$$

to rewrite the recursion of Eq. (1) as

$$z_{n+1} = \frac{z_n^{(1)} z_n^{(2)} + b - 1}{b}. \tag{7}$$

A. Reminder of the pure case

In the pure case, the ratios z_n defined in Eq. (6) are not random but take a single value R_n, and the recursion of Eq. (7) reduces to a one-dimensional mapping T

$$R_{n+1} = \frac{R_n^2 + b - 1}{b} \equiv T(R_n) \tag{8}$$

discussed in Ref. [11]: for $b>2$, there exists two attractive fixed points $R_\infty = 1$ (delocalized phase) and $R_\infty = +\infty$ (localized phase) separated by the repulsive fixed point R_c (critical point) with

$$R_c = b - 1. \tag{9}$$

The critical exponents are determined by the linearization of the recurrence around the fixed point. Setting $R_n = R_c + \delta_n$, one obtains at linear order

$$\delta_{n+1} \simeq \lambda \delta_n \quad \text{with} \quad \lambda = T'(R_c) = \frac{2R_c}{b} = \frac{2(b-1)}{b}. \tag{10}$$

Note that this factor $\lambda = T'(R_c) > 1$ describing the instability of the critical point also governs the growing of the energy E_n exactly at criticality [20], since the recursion for the energy

$$E_{n+1} = \frac{R_n^2 (2E_n)}{R_n^2 + b - 1} \tag{11}$$

becomes at criticality

$$E_{n+1}(T_c) = \frac{2R_c^2}{R_c^2 + b - 1} E_n(T_c) = \lambda E_n(T_c). \tag{12}$$

To understand why the same factor λ appears, one may introduce the product $U_n = R_n E_n$ that satisfies the recursion

$$U_{n+1} = \frac{2R_n}{b} U_n. \tag{13}$$

It is then clear that at criticality it coincides with the recursion of the variables δ_n [Eq. (10)].

In conclusion, the variable δ_n or the energy E_n at criticality grows as $\lambda^n = L_n^{1/\nu}$ in terms of the length $L_n = 2^n$ with the critical exponent

$$\nu = \frac{\ln 2}{\ln \lambda} = \frac{\ln 2}{\ln T'(R_c)}. \tag{14}$$

The specific heat exponent satisfies the hyperscaling relation $\alpha = 2 - \nu$. We refer to Ref. [11] for more details.

Let us now summarize the changes that the presence of frozen disorder will induce. (i) The one-dimensional mapping of the pure case $R_{n+1} = T(R_n)$ will become the iteration of a probability distribution $Q_{n+1}(z) = \mathcal{F}\{Q_n(z)\}$. (ii) The critical value R_c of the pure case will become an invariant probability distribution $Q_c(z) = \mathcal{F}\{Q_c(z)\}$. (iii) The critical expo-

nent ν determined by the derivative $T'(R_c)$ in the pure case will be determined by the linearized iteration around the fixed point distribution $Q_c(z)$. However, before concentrating on the critical point, we first describe the properties of the renormalization group (RG) flow with disorder in the limits of high and low temperatures.

B. High-temperature RG flow

In the high-temperature phase, the variables z_n defined in Eq. (6) flow toward 1 or equivalently the free-energies f_n decay to zero. The linearization of the recursion in this regime yields

$$f_{n+1} \simeq \frac{f_n^{(1)} + f_n^{(2)}}{b}. \tag{15}$$

For $b>2$, this high-temperature phase exists, the probability distribution of the free-energy converges to a Gaussian, and the average and the width decay as power laws of the length $L_n=2^n$:

$$\overline{f_n} \propto L_n^{-[\ln (b/2)/\ln 2]}, \tag{16}$$

$$\sqrt{\overline{f_n^2} - (\overline{f_n})^2} \propto L_n^{-\omega'_W(b)} \quad \text{with} \quad \omega'_W(b) = \frac{\ln \frac{b^2}{2}}{2 \ln 2}. \tag{17}$$

C. Low-temperature RG flow

In the low-temperature phase, the free-energies f_n of Eq. (6) grow extensively with the length $L_n=2^n$, and thus at large scale, the recursion is dominated by the first term in Eq. (7)

$$f_{n+1} \simeq f_n^{(1)} + f_n^{(2)} + \cdots . \tag{18}$$

The probability distribution of the free-energy thus converges to a Gaussian, the average and the width grows as

$$\overline{f_n} \propto L_n, \tag{19}$$

$$\sqrt{\overline{f_n^2} - (\overline{f_n})^2} \propto L_n^{1/2}. \tag{20}$$

D. Analysis of the critical invariant distribution

At criticality, to avoid the high-temperature and low-temperature described above, the free energy f_n of Eq. (6) should remain a random variable of order $O(1)$ with some scale-invariant probability distribution $P_c(f)$ defined on $]-\infty,0]$. Equivalently, the variable $z_n=e^{-\beta_c f_n}$ should have a scale-invariant probability distribution $Q_c(z)$ defined on $[1,+\infty[$. In the following, we derive some of their properties.

1. Left-tail behavior of the free-energy distribution

Let us introduce the left-tail exponent η_c

$$\ln P_c(f) \underset{f\to-\infty}{\simeq} -\gamma(-f)^{\eta_c} + \cdots, \tag{21}$$

where $(\cdots)$ denote the subleading terms. In the region where $f\to-\infty$, one has effectively the low-temperature recursion

$$f \simeq f^{(1)} + f^{(2)} + \cdots . \tag{22}$$

A saddle-point analysis shows that if $f^{(1)}$ and $f^{(2)}$ have a probability distribution with the left tail given by Eq. (21), their sum f has for left tail $\ln P_c(f) \simeq -\gamma(-f)^{\eta_c} 2^{1-\eta_c} + \cdots$. The stability of the critical distribution thus fixes the value of the left tail exponent to

$$\eta_c = 1. \tag{23}$$

So the distribution $P_c(f)$ decays exponentially

$$P_c(f) \underset{f\to-\infty}{\simeq} e^{\gamma f}(\cdots). \tag{24}$$

This means that the corresponding distribution $Q_c(z)$ of $z=e^{-\beta_c f}$ presents a power-law tail

$$Q_c(z) \underset{z\to+\infty}{\simeq} \frac{\Phi(\ln z)}{z^{1+\mu}} \tag{25}$$

with some exponent

$$\mu = \frac{\gamma}{\beta_c} \tag{26}$$

and where $\Phi(\ln z)$ represents the subleading terms.

2. Analysis in terms of multiplicative stochastic processes

The fact that a power-law appears in the stationary distribution of some random iteration is reminiscent of multiplicative stochastic processes, whose main properties are recalled in the Appendix. For a multiplicative stochastic process X_n described by Eq. (A1), the stationary distribution presents a power-law tail of exponent μ that can be computed in terms of the statistics of the random coefficient a_n via Eq. (A4). Here, for the quadratic renormalization of Eq. (7), it is the process z_n itself that also plays the role of the random multiplicative coefficient. As a consequence, it is instructive to analyze the recursion of Eq. (7) along the same lines used to study multiplicative stochastic processes.

The necessary stability condition of Eq. (A2) translates here into the following condition:

$$\overline{\ln \frac{z}{b}} \equiv \int_1^{+\infty} dz Q_c(z) \ln z - \ln b < 0. \tag{27}$$

The condition of Eq. (A4) that ensures the stability of the power-law tail via iteration translates into the following self-consistent condition for the tail exponent μ introduced in Eq. (25):

$$2\overline{\left(\frac{z}{b}\right)^{\mu}} \equiv 2\int_1^{+\infty} dz Q_c(z) \left(\frac{z}{b}\right)^{\mu} = 1. \tag{28}$$

The argument is similar to the computation of Eqs. (A5) and (A6), the additional factor of 2 coming from the fact that z large corresponds to either $z^{(1)}$ large or $z^{(2)}$ large. The condition of Eq. (28) means in particular that the subleading term $\Phi(\ln z)$ in Eq. (25) should ensure the convergence at $(+\infty)$ of the following integral:

$$\overline{z^{\mu}} = \int^{+\infty} dz Q_c(z) z^{\mu} \sim \int^{+\infty} \frac{dz}{z} \Phi(\ln z) \sim \int^{+\infty} dw \Phi(w) < +\infty. \quad (29)$$

Since Φ is a subleading term in Eq. (25), it should not contain an exponential, so its decay should be a power law

$$\Phi(w) \underset{w \to \infty}{\simeq} \frac{1}{w^{1+\sigma}} \quad \text{with} \quad \sigma > 0. \quad (30)$$

Then moments of order $k \leq \mu$ are finite, whereas moments of order $k > \mu$ diverge

$$\int^{+\infty} dz Q_c(z) z^k = +\infty \quad \text{for} \quad k > \mu. \quad (31)$$

In contrast with multiplicative stochastic processes where the condition of Eq. (A4) allows one to compute the tail exponent μ in terms of the known statistics of the random coefficient a_n, we have obtained here only a self-consistent equation: The selected tail exponent μ in the region $z \to \infty$ is the exponent that satisfies the condition of Eq. (28) that involves the whole distribution for $z \in (1, +\infty[$. However, even if we cannot explicitly compute this exponent μ, we can try to locate it with respect to integer values by considering the integer moments.

3. Reminder on transitions of integer moments

An important property of quadratic renormalizations is that they lead to closed renormalizations for the integer moments. We now briefly recall the behavior of the first moments discussed in Ref. [11]. The closed recursion satisfied by the first moment [11]

$$\overline{z_{n+1}} = \frac{(\overline{z_n})^2 + b - 1}{b} \quad (32)$$

coincides with the pure case equation of Eq. (8). Using the initial condition of Eq. (4), the unstable fixed point of Eq. (9) allows one to define the annealed temperature via $e^{-\epsilon_i / T_{\rm ann}} = b - 1$: for $T > T_{\rm ann}$, the averaged value $\overline{z_n}$ goes to 1, whereas for $T < T_{\rm ann}$, the averaged value $\overline{z_n}$ goes to $+\infty$. So $T_{\rm ann}$ represents the transition of the first moment. To locate T_c with respect to $T_{\rm ann}$, we have to distinguish two possibilities. (i) If the tail exponent μ of Eq. (25) satisfies $0 < \mu < 1$, then its first moment diverges at criticality $\overline{z_c} = +\infty$ and we have the strict inequality $T_c < T_{\rm ann}$. (ii) If the tail exponent μ satisfies $\mu > 1$, then its first moment is finite at criticality. The only possible finite stable value is $\overline{z_c} = b - 1$ and the critical temperature then coincides with the annealed temperature $T_c = T_{\rm ann}$. However, the analysis of the recursion for the variance leads to the conclusion that the critical temperature is strictly lower than the annealed temperature $T_c < T_{\rm ann}$ as soon as disorder is relevant $b \geq 2 + \sqrt{2} \simeq 3.414$ [11]. In conclusion, whenever disorder is relevant at criticality, one has the strict inequality $T_c < T_{\rm ann}$, the first moment diverges $\overline{z_c} = +\infty$, and the tail exponent μ of Eq. (25) is smaller than 1:

$$0 < \mu < 1. \quad (33)$$

E. Critical exponent ν

1. Equivalence with a directed polymer on a Cayley tree

In the pure case, the critical exponents are obtained from the linearization around the fixed point (see Sec. II A). To follow the same strategy in the disordered case, we set $z_n = z_c + \delta_n$. At linear order, we obtain the recursion

$$\delta_{n+1} \simeq \frac{z_c^{(1)}}{b} \delta_n^{(2)} + \frac{z_c^{(2)}}{b} \delta_n^{(1)}, \quad (34)$$

where $z_c^{(1,2)}$ are distributed with the critical distribution $Q_c(z)$. As in the pure case, it is also interesting to write the recursion for the energy E_n

$$E_{n+1} \simeq \frac{z_c^{(1)} z_c^{(2)} (E_n^{(1)} + E_n^{(2)})}{z_c^{(1)} z_c^{(2)} + b - 1} \quad (35)$$

so that the combination $U_n \equiv z_n E_n$ satisfies at criticality the same recursion as in Eq. (34)

$$U_{n+1} = \frac{z_c^{(1)}}{b} U_n^{(2)} + \frac{z_c^{(2)}}{b} U_n^{(1)}. \quad (36)$$

The recurrence of Eq. (34) coincides with the transfer matrix

$$Z_{L+1} = \sum_{i=1}^{K} e^{-\epsilon_i} Z_L^{(i)} \quad (37)$$

for the partition function Z_L of a directed polymer on a Cayley tree of branching ratio $K=2$ with random bond energies ϵ_i [23,24]. The differences with Eq. (34) we are interested in are the following: (i) The partition function Z_L in Eq. (37) is positive by definition, whereas here the random perturbation δ_n in Eq. (34) are *a priori* of arbitrary sign. Equation (34) is thus more related to the case of a directed polymer model with complex weights studied in Ref. [25]. (ii) The weights $e^{-\beta \epsilon_i}$ associated to the bond energies ϵ_i in Eq. (37) are now random weights $\frac{z_c}{b}$ distributed with the fixed point distribution $Q_c(z)$

$$e^{-\beta \epsilon_i} \to \frac{z_c}{b}. \quad (38)$$

In particular, these weights present a broad power-law tail in $1/z_c^{1+\mu}$ in contrast with the usual case where the energies ϵ_i are Gaussian. The difference (ii) turns out to be very important as we now explain.

2. Tails analysis

Let us consider the first iteration

$$\delta_1 = \frac{z_c^{(1)}}{b} \delta_0^{(2)} + \frac{z_c^{(2)}}{b} \delta_0^{(1)}. \quad (39)$$

Suppose we start with a narrow distribution $\mathcal{P}_0(\delta_0)$ for the random initial perturbation δ_0. The distribution $\mathcal{P}_1(\delta_1)$ after

the first iteration will nevertheless present power-law tails inherited from the fixed point distribution $Q_c(z_c) \sim \Phi(\ln z_c)/z_c^{1+\mu}$ with $0<\mu<1$ [Eqs. (25) and (33)]. More precisely, the tail in the region $\delta_1 \to +\infty$ is dominated by the events where $z_c^{(1)}$ is large with $\delta_0^{(2)}>0$ or where $z_c^{(2)}$ is large with $\delta_0^{(1)}>0$, and one obtains

$$\mathcal{P}_1(\delta_1) \underset{\delta_1\to+\infty}{\simeq} 2\int dz_c Q_c(z_c) \int_0^{+\infty} d\delta_0 \mathcal{P}_0(\delta_0)\delta\left[\delta_1 - \frac{z_c}{b}\delta_0\right] \tag{40}$$

$$\underset{\delta_1\to+\infty}{\simeq} \frac{\Phi(\ln \delta_1)}{\delta_1^{1+\mu}}\left[\frac{2}{b^\mu}\int_0^{+\infty} d\delta_0 \mathcal{P}_0(\delta_0)\delta_0^\mu\right]. \tag{41}$$

Similarly, the left tail reads

$$\mathcal{P}_1(\delta_1) \underset{\delta_1\to-\infty}{\simeq} \frac{\Phi(\ln|\delta_1|)}{|\delta_1|^{1+\mu}}\left[\frac{2}{b^\mu}\int_{-\infty}^{0} d\delta_0 \mathcal{P}_0(\delta_0)|\delta_0|^\mu\right]. \tag{42}$$

It is then clear that by iteration all distributions $\mathcal{P}_n(\delta_n)$ will present these power-law tails

$$\mathcal{P}_n(\delta_n) \underset{\delta_n\to\pm\infty}{\propto} \frac{\Phi(\ln|\delta_n|)}{|\delta_n|^{1+\mu}}. \tag{43}$$

Since we are looking for the Lyapunov exponent v governing the typical growth of the perturbation

$$\frac{\delta_{n+1}}{\delta_n} \sim e^v \tag{44}$$

it is convenient to rescale the iteration of Eq. (34) by the factor e^{-v}

$$y_{n+1} = e^{-v}\left[\frac{z_c^{(1)}}{b}y_n^{(2)} + \frac{z_c^{(2)}}{b}y_n^{(1)}\right] \tag{45}$$

and to ask that the probability distribution $P_n(y)$ converges as $n\to\infty$ toward a stable distribution $P_\infty(y)$ presenting the tails [Eq. (43)]

$$P_\infty(y) \underset{y\to\pm\infty}{\simeq} B^\pm \frac{\Phi(\ln|y|)}{|y|^{1+\mu}}. \tag{46}$$

Reasoning as before, a large value of y_{n+1} corresponds to a large value of one of the four variables $(y_n^{(1)}, y_n^{(2)}, z_c^{(1)}, z_c^{(2)})$, and one obtains the following equations

$$B^+ = \left[B^+\frac{2e^{-\mu v}\overline{z_c^\mu}}{b^\mu} + \frac{2e^{-\mu v}}{b^\mu}\int_0^{+\infty} dy P_\infty(y) y^\mu\right], \tag{47}$$

$$B^- = \left[B^-\frac{2e^{-\mu v}\overline{z_c^\mu}}{b^\mu} + \frac{2e^{-\mu v}}{b^\mu}\int_{-\infty}^{0} dy P_\infty(y) |y|^\mu\right]. \tag{48}$$

This shows that positive perturbations [initial distribution $\mathcal{P}_0(\delta_0<0)=0$] or symmetric perturbations [symmetric initial distribution $\mathcal{P}_0(\delta_0)=\mathcal{P}_0(-\delta_0)$] actually lead to the same Lyapunov exponent v

$$e^{\mu v} = \frac{2\overline{z_c^\mu}}{b^\mu} + \frac{2}{b^\mu}\int_0^{+\infty} dy \frac{P_\infty(y)}{B_+} y^\mu = 1 + \frac{2}{b^\mu}\int_0^{+\infty} dy \frac{P_\infty(y)}{B_+} y^\mu, \tag{49}$$

where we have used Eq. (28). The first term corresponds to the usual term for the velocity of the traveling wave approach [23,24], whereas the second term originates from the broad distribution of weights (z_c/b). Its physical meaning is the following: In the usual case of a narrow distribution of the weights, the traveling wave approach allows one to compute the velocity in terms of the weight statistics alone, because one can write a closed equation for the tail of the process [23,24]; in the present case, the tail of the process does not satisfy a closed equation because the broadness of the weight distribution induces some interaction between the tail and the bulk of the process: the second term in Eq. (49) represents the influence of the bulk of the distribution $P_\infty(y)$ onto the tail of exponent μ.

The exponent ν describing the power-law growth $\delta_n \sim L_n^{1/\nu} \sim e^{vn}$ reads in terms of the Lyapunov exponent

$$\nu = \frac{\ln 2}{v}. \tag{50}$$

Note that the presence of the second term in Eq. (49) is crucial to obtain a finite exponent ν: without this second term, the Lyapunov exponent v would vanish $(v=0)$ and the correlation length exponent would diverge $(\nu=\infty)$.

III. NUMERICAL STUDY OF THE WETTING TRANSITION

A. Numerical method

We have performed numerical simulations with the so-called "pool-method" which is very much used for disordered systems on hierarchical lattices [10,14]: the idea is to represent the probability distribution $P_n(F_n)$ of the free-energy $F_n=-T\ln Z_n$ at generation n, by a pool of N values $\{F_n^{(1)},\ldots,F_n^{(N)}\}$. The pool at generation $(n+1)$ is then obtained as follows: Each value $F_{n+1}^{(i)}$ is obtained by choosing two values at random from the pool of generation n and by applying the renormalization Eq. (7).

The results presented in this section have been obtained for the branching ratio $b=5$, with a pool number $N=4\times10^7$, with initial Gaussian energies [Eq. (3)]. The corresponding annealed temperature is

$$T_{\text{ann}} = \frac{1}{\sqrt{2\ln(b-1)}} \simeq 0.600\,55. \tag{51}$$

Finally, the relation between the true free-energy $F_n=-T\ln Z_n$ and the reduced free-energy $f_n=-T\ln z_n$ used in the previous section is simply [Eq. (6)]

$$F_n = f_n - T\ln Y_n, \tag{52}$$

where $Y_n=b^{L_n-1}$ does not contain any disorder. As a consequence, the two free-energy distributions have the same width $\Delta F_n=\Delta f_n$, and the same tail properties.

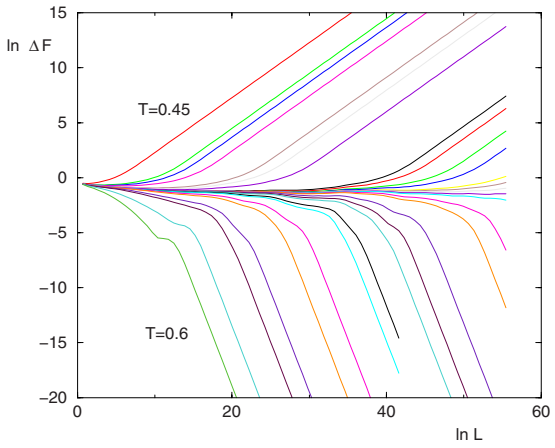

FIG. 2. (Color online) Wetting transition: log-log plot of the width $\Delta F(L)$ of the free-energy distribution as a function of L, for many temperatures.

B. Flow of the free-energy width ΔF_L

The flow of the free-energy width ΔF_L as L grows is shown on Fig. 2 for many temperatures. One clearly sees the two attractive fixed points on this log-log plot.

For $T>T_c$, the free-energy width decays asymptotically with the exponent $\omega'_W(b)$ introduced in Eq. (17)

$$\Delta F(L) \simeq \left(\frac{L}{\xi_F^+(T)}\right)^{-\omega'_W(b=5)}$$

$$\text{with} \quad \omega'_W(b=5) = \frac{\ln(b^2/2)}{2\ln 2} = 1.8219, \quad (53)$$

where $\xi_F^+(T)$ is the corresponding correlation length that diverges as $T \to T_c^+$. For $T<T_c$, the free-energy width grows asymptotically with the exponent 1/2 [see Eq. (20)]

$$\Delta F(L) \simeq \left(\frac{L}{\xi_F^-(T)}\right)^{1/2}, \quad (54)$$

where $\xi_F^-(T)$ is the corresponding correlation length that diverges as $T \to T_c^-$.

The critical temperature obtained by this pool method depends of the pool, i.e., of the discrete sampling with N values of the continuous probability distribution. It is expected to converge toward the thermodynamic critical temperature T_c only in the limit $N \to \infty$. Nevertheless, for each given pool, the flow of free-energy width allows a very precise determination of this pool-dependent critical temperature, for instance, in the case considered $0.524\,15 < T_c^{\text{pool}} < 0.524\,16$, which is significantly below the annealed temperature of Eq. (51).

C. Divergence of the correlation lengths $\xi_F^{\pm}(T)$

The correlation lengths $\xi_F^{\pm}(T)$ as measured from the free-energy width asymptotic behaviors above and below T_c [Eqs. (53) and (54)] are shown in Fig. 3(a). The plot in terms of the variable $\ln|T_c - T|$ shown on Fig. 3(b) indicate a power-law divergence with the same exponent

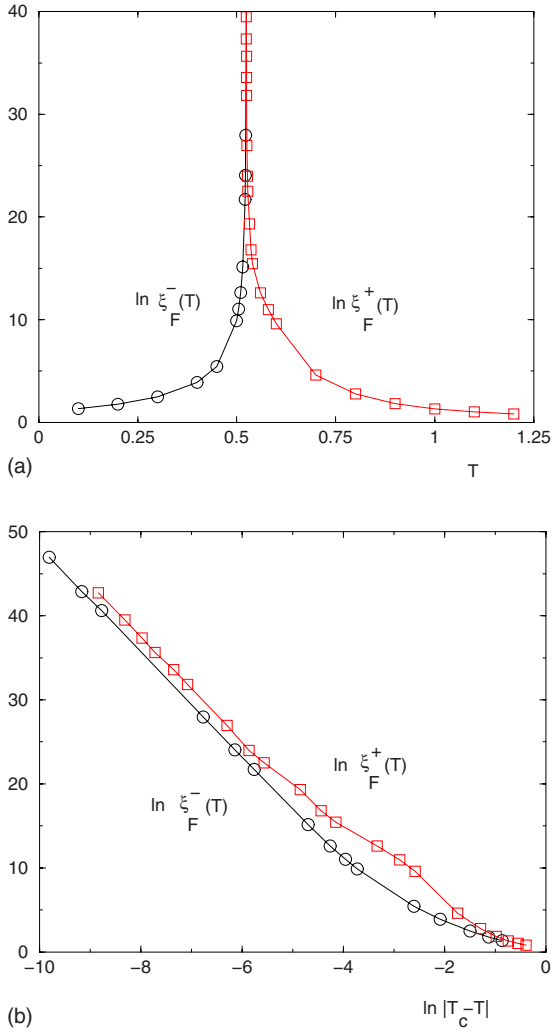

FIG. 3. (Color online) Wetting transition: Correlation length $\xi_F^{\pm}(T)$ as measured from the behavior of the free-energy width [Eqs. (53) and (54)]. (a) $\ln \xi_F^{\pm}(T)$ as a function of T. (b) $\ln \xi_F^{\pm}(T)$ as a function of $\ln|T_c - T|$: the asymptotic slopes are of order $\nu \sim 6.2$.

$$\xi_F^{\pm}(T) \underset{T \to T_c}{\propto} |T - T_c|^{-\nu} \quad \text{with} \quad \nu \simeq 6.2. \quad (55)$$

D. Histogram of the free-energy

The asymptotic probability distribution Π_F of the rescaled free-energy

$$x_F \equiv \frac{F - F_{\text{av}(L)}}{\Delta F(L)} \quad (56)$$

is shown in Fig. 4 for three temperatures. (i) The distribution is Gaussian both for $T>T_c$ and $T<T_c$ as expected from Eqs. (15) and (18). (ii) At criticality, one clearly sees that a left-tail develops in the region $f \to -\infty$ with tail exponent $\eta_c = 1$ in agreement with Eq. (23). The corresponding power-law exponent of Eq. (26) of the fixed-point distribution of Eq. (25) is of order

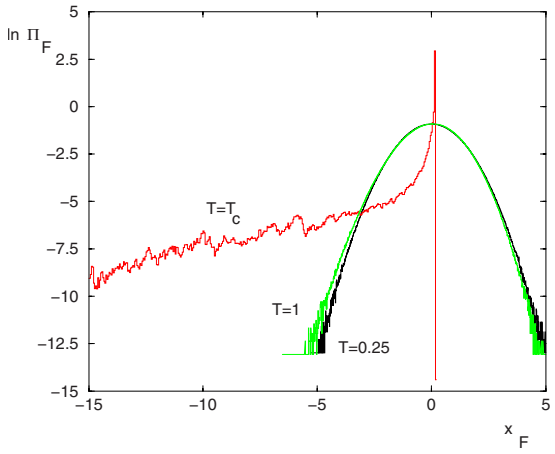

FIG. 4. (Color online) Wetting transition: Log-plot of the asymptotic distribution Π_F of the rescaled free-energy $x_F = \frac{F - F_{\mathrm{av}(L)}}{\Delta F(L)}$ in the low-temperature phase (here $T=0.25$), in the high-temperature phase (here $T=1$) and at criticality (here $T_c^{\mathrm{pool}} = 0.524\,155$).

$$\mu \sim 0.45. \tag{57}$$

The measure is not very precise because one clearly sees on Fig. 4 that on top of this power law, there exists oscillations reflecting the discrete nature of the renormalization. However, this value is in the expected interval of Eq. (33).

E. Flow of the energy width

The flow of the energy width $\Delta E(L)$ as L grows are shown on Fig. 5 for many temperatures. For $T > T_c$, we find that the width decays asymptotically with the same exponent $\omega_\infty^W(b)$ as the free energy [Eq. (53)]

$$\Delta E(L) \simeq L^{-\omega_\infty^W(b)} \quad \text{with} \quad \omega_\infty^W(b=5) = \frac{\ln(b^2/2)}{2\ln 2} = 1.8219. \tag{58}$$

For $T < T_c$, this width grows asymptotically with the exponent 1/2 as the free energy [Eq. (54)]

$$\Delta E(L) \simeq L^{1/2}. \tag{59}$$

Exactly at criticality, the free-energy $\Delta F(L)$ width converges toward a constant, whereas the energy width grows as a power law [see Fig. 5(b)]

$$\Delta E(L) \simeq L^{y_c} \quad \text{with} \quad y_c \simeq 0.16. \tag{60}$$

This exponent is in agreement with the finite-size scaling relation $y_c = 1/\nu$ with $\nu \simeq 6.2$ [see Eq. (55)].

IV. DIRECTED POLYMER MODEL ON DIAMOND HIERARCHICAL LATTICES

In this section we study the directed polymer model, whose partition function satisfies the quadratic renormalization of Eq. (5). In contrast with the wetting case described above, the transition only exists in the presence of disorder. Since we are interested into the asymptotic distribution of the

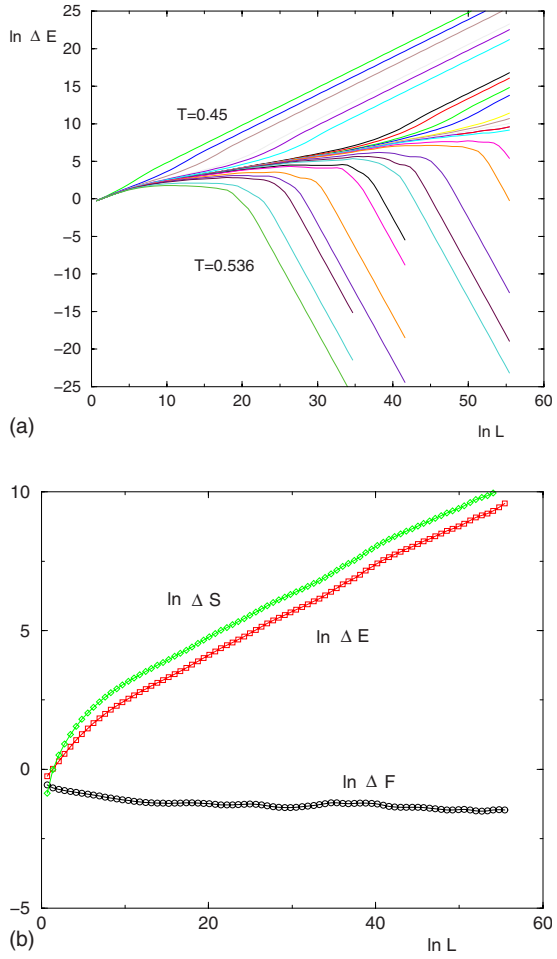

FIG. 5. (Color online) Wetting transition: Flow of the widths $\Delta E(L)$ of the energy distribution as L grows. (a) $\ln \Delta E(L)$ as a function of $\ln L$ for many temperatures. (b) Comparison of $\ln \Delta E(L)$, $\ln \Delta S(L)$, and $\ln \Delta F(L)$ as a function of $\ln L$ at criticality ($T_c^{\mathrm{pool}} = 0.524\,155$).

free energy, it is convenient to rewrite the free energy $F_n^{(a)}$ of a sample (a) of generation n as

$$F_n^{(a)} \equiv \ln Z_n^{(a)} = \overline{F_n} + \Delta_n u_a, \tag{61}$$

where u_a is a random variable of zero mean and width unity

$$\overline{u_a^2} = 1. \tag{62}$$

So Δ_n represents the width

$$\Delta_n = [\overline{F_n^2} - (\overline{F_n})^2]^{1/2}. \tag{63}$$

A. Low-temperature RG flow

In the low-temperature phase, the width Δ_n of the free-energy distribution grows with n. So at large scale, the recursion is dominated by the maximal term in Eq. (5)

$$F_{n+1} \simeq \min_{1 \le a \le b} (F_n^{(2a-1)} + F_n^{(2a)}). \tag{64}$$

This effective low-temperature recursion coincides with the recursion of the energy E_0 of the ground state studied in

Refs. [13,14]. The whole low-temperature phase is thus described by the zero-temperature fixed point. In particular, the width of the free-energy distribution grows as

$$\Delta_n \simeq L_n^{\omega_0(b)}, \tag{65}$$

where $\omega_0(b)$ is the exponent governing the width of the ground-state energy $\Delta E_0 \sim L_n^{\omega_0(b)}$ studied in Ref. [13].

B. High-temperature RG flow

In the high-temperature phase, the width Δ_n of the free-energy distribution is expected to decay to zero. The linearization in Δ_n of the recursion of Eq. (5) yields

$$\beta F_{n+1} = -\ln\left[\sum_{a=1}^{b} e^{-\beta(F_n^{(2a-1)}+F_n^{(2a)})}\right]$$

$$= 2\beta\overline{F_n} - \ln[b - \beta\Delta_n \sum_{a=1}^{b}(u_{2a-1}+u_{2a}) + O(\beta^2\Delta_n^2)] \tag{66}$$

$$= 2\beta\overline{F_n} - \ln(b) + \frac{\beta\Delta_n}{b}\sum_{a=1}^{b}(u_{2a-1}+u_{2a}) + O(\beta^2\Delta_n^2). \tag{67}$$

The consistence with the scaling form of Eq. (61) at generation $(n+1)$

$$F_{n+1} = \overline{F_{n+1}} + \Delta_{n+1}u \tag{68}$$

yields

$$\overline{F_{n+1}} = 2\overline{F_n} - T\ln(b),$$

$$\Delta_{n+1}u = \frac{\Delta_n}{b}\sum_{a=1}^{b}(u_{2a-1}+u_{2a}). \tag{69}$$

The normalization condition of Eq. (62) yields

$$\Delta_{n+1} = \sqrt{\frac{2}{b}}\Delta_n \tag{70}$$

and

$$u = \frac{1}{\sqrt{2b}}\sum_{a=1}^{b}(u_{2a-1}+u_{2a}). \tag{71}$$

For $b>2$, this high-temperature phase exists, the probability distribution of the free-energy converges to a Gaussian. The width decays as the following power-law of the length $L_n = 2^n$

$$\Delta_n \propto L_n^{-\omega_\infty(b)} \quad \text{with} \quad \omega_\infty(b) = \frac{\ln\frac{b}{2}}{2\ln 2}. \tag{72}$$

In this regime, the rescaled variable u evolves according to Eq. (71) and thus becomes Gaussian upon iteration.

C. Analysis of the critical point

At criticality, to avoid the high-temperature and low-temperature described above, the width Δ_n should converge as $n\to\infty$ toward a finite value Δ_c. In particular, the fluctuating part of the free energy

$$f_n^{(a)} \equiv F_n^{(a)} - \overline{F_n} = \Delta_c u^{(a)} \tag{73}$$

should remain a random variable of order $O(1)$, of zero mean, distributed with some scale-invariant probability distribution $P_c(f)$ defined on $]-\infty,+\infty[$. Equivalently, the variable

$$z_n^{(a)} \equiv e^{-\beta_c f_n^{(a)}} = e^{-\beta_c\Delta_c u^{(a)}} \tag{74}$$

should have a scale-invariant probability distribution $Q_c(z)$ defined on $[0,+\infty[$, with

$$\overline{\ln z} = \int_0^{+\infty} dz\, \ln z Q_c(z) = 0. \tag{75}$$

The recursion for these variables z_n reads

$$z_{n+1} = \frac{1}{\mathcal{B}}\sum_{a=1}^{b} z_n^{(2a-1)} z_n^{(2a)}, \tag{76}$$

where

$$\mathcal{B} \equiv \lim_{n\to\infty}(\overline{F_{n+1}} - 2\overline{F_n}) \tag{77}$$

should be finite [otherwise the recursion of Eq. (76) would not lead to a non-trivial stationary distribution $Q_c(z)$].

1. Left-tail behavior of the free-energy distribution

Let us introduce the left-tail exponent η_c

$$\ln P_c(f) \underset{f\to-\infty}{\simeq} -\gamma(-f)^{\eta_c} + \cdots, \tag{78}$$

where $(\cdots)$ denote the subleading terms. In the region where $f\to-\infty$, one has effectively the low-temperature recursion of Eq. (64)

$$f \simeq \min_{1\le a\le b}(f^{(2a-1)} + f^{(2a)}). \tag{79}$$

As in the wetting case, a saddle-point analysis shows that the only stable left tail exponent is

$$\eta_c = 1. \tag{80}$$

So the distribution $P_c(f)$ decays exponentially

$$P_c(f) \underset{f\to-\infty}{\simeq} e^{\gamma f}(\cdots). \tag{81}$$

This means that the corresponding distribution $Q_c(z)$ of $z = e^{-\beta_c f}$ presents a power-law tail

$$Q_c(z) \underset{z\to+\infty}{\simeq} \frac{\Phi(\ln z)}{z^{1+\mu}} \tag{82}$$

with some exponent

$$\mu = \frac{\gamma}{\beta_c} \tag{83}$$

and where $\Phi(\ln z)$ represents the subleading terms.

The first moment is fixed by the recursion of Eq. (76)

$$\bar{z} = \frac{\mathcal{B}}{b}. \tag{84}$$

As a consequence, the exponent μ of the power law of Eq. (82) should satisfy

$$\mu > 1 \tag{85}$$

and the parameter $\mathcal{B}$ representing the correction to extensivity [Eq. (77)] is determined by

$$\mathcal{B} = b\bar{z} = b\int dz z Q_c(z) \tag{86}$$

in terms of the fixed point distribution $Q_c(z)$.

2. Analysis in terms of multiplicative stochastic processes

Again, as explained in Sec. II D 2, it is instructive to analyze the recursion of Eq. (76) from the point of view of multiplicative stochastic processes (see the Appendix). The condition of Eq. (A2) translates here into the following condition using Eq. (75)

$$\overline{\ln \frac{z}{\mathcal{B}}} = -\ln \mathcal{B} = -\ln(b\bar{z}) < 0 \tag{87}$$

The condition of Eq. (A4) translates into the following condition for the exponent μ introduced in Eq. (82):

$$2b\overline{\left(\frac{z}{\mathcal{B}}\right)^{\mu}} = \frac{2}{b^{\mu-1}}\frac{\overline{z^{\mu}}}{(\bar{z})^{\mu}} \equiv \frac{2}{b^{\mu-1}}\frac{\int_0^{+\infty} dz Q_c(z) z^{\mu}}{\left[\int_0^{+\infty} dz Q_c(z) z\right]^{\mu}} = 1. \tag{88}$$

The argument is similar to Eqs. (A5) and (A6), the additional factor of $2b$ coming from the fact that z large corresponds to one of the $z^{(i)}$ being large. This condition means in particular that the subleading term $\Phi(z)$ in Eq. (25) should ensure the convergence at $(+\infty)$ as in the wetting case [see Eqs. (29) and (31)].

3. Reminder on transitions of integer moments

Let us now briefly recall the behaviors of the first moments discussed in Ref. [14]. From Eq. (5), one obtains [14]

$$\overline{Z_{n+1}} = b(\overline{Z_n})^2, \tag{89}$$

$$\overline{Z_{n+1}^2} = b(\overline{Z_n^2})^2 + b(b-1)(\overline{Z_n})^4, \tag{90}$$

so that the ratio of the moments of the rescaled variable z defined in Eq. (74)

$$r_2(n) \equiv \frac{\overline{Z_n^2}}{(\overline{Z_n})^2} = \frac{\overline{z_n^2}}{(\overline{z_n})^2} \tag{91}$$

follows the closed recursion [14]

$$r_2(n+1) = \frac{r_2^2(n) + b - 1}{b} \tag{92}$$

that actually coincides with Eq. (8) for the pure wetting model. The repulsive fixed point $r^* = b-1$ allows one to define the temperature T_2 via $r_2(n=0) = b-1$ [14]: For $T > T_2$, the ratio $r_2(n)$ flows to 1, whereas for $T > T_2$, the ratio $r_2(n)$ flows to $(+\infty)$. Similarly, the RG flow of ratios corresponding to higher moments have been studied in Ref. [14], with the conclusion that for generic b (more precisely $b > 2.303\ldots$) their transition temperatures are higher than T_2.

Since we already know $\mu > 1$ [Eq. (85)], we have to distinguish two cases. (i) If the tail exponent μ satisfies $1 < \mu < 2$, then the second moment diverges at criticality $\overline{z^2} = +\infty$ and we have the strict inequality $T_c < T_2$. (ii) if the tail exponent μ satisfies $\mu > 2$, then the second moment is finite at criticality. The only possible finite stable value is for the ratio r_2 is $r_2 = b-1$. The critical temperature then coincides with the transition temperature of the second moment $T_c = T_2$. The scenario (i) is the most plausible, since the possibility (ii) would require some "fine-tuning" in some sense: as explained in the introduction, the temperature only appears in the initial condition [Eq. (4)] of the renormalization; any initial temperature $T > T_c$ flows toward the high-temperature fixed point, any initial temperature $T < T_c$ flows toward the low-temperature fixed point, so that T_c is defined as the only initial temperature from which the critical distribution $Q_c(z)$ is accessible. The critical distribution $Q_c(z)$ has to satisfy the self-consistent equation of Eq. (87) to be stable. If (ii) were true, the distribution $Q_c(z)$ should in addition satisfy a second completely independent condition $r_2 = b-1$, which seems unlikely.

In conclusion, we expect that the exponent μ introduced in Eq. (82) satisfies

$$1 < \mu < 2. \tag{93}$$

This is in agreement with the numerical simulations presented below in Sec. V.

4. Right tail behavior of the free-energy distribution

Let us introduce the right-tail exponent η_c

$$\ln P_c(f) \underset{f \to +\infty}{\simeq} -\gamma' f^{\eta_c'} + \cdots. \tag{94}$$

In the region where $f \to +\infty$, one has effectively the high-temperature recursion

$$f \simeq \frac{1}{b}\sum_{i=1}^{2b} f^{(i)}, \tag{95}$$

where all free energies are large. A saddle-point analysis with the right tail of Eq. (94) shows that the only stable right exponent η_c' should satisfy $b = 2^{\eta_c' - 1}$, i.e.,

$$\eta_c' = 1 + \frac{\ln b}{\ln 2}. \tag{96}$$

D. Critical exponent ν

To compute the critical exponent ν, we consider a small perturbation in the fluctuating part of the free-energy of Eq. (73)

$$-\beta_c f_n^{(a)} \equiv -\beta_c (F_n^{(a)} - \overline{F_n}) = -\beta \Delta_c u^{(a)} + \delta_n^{(a)}, \quad (97)$$

where $\delta_n^{(a)}$ represent the random perturbations of zero mean

$$\overline{\delta_n} = 0. \quad (98)$$

Equivalently, these variables δ_n represent the perturbation at linear order of the variables of Eq. (74)

$$z_n^{(a)} \equiv e^{-\beta_c f_n^{(a)}} = z_c^{(a)} + \delta_n^{(a)}. \quad (99)$$

The linearization of the recursion of Eq. (76) around the fixed point, yields

$$\delta_{n+1} \simeq \sum_{i=1}^{2b} \frac{z_c^{(i)}}{\mathcal{B}} \delta_n^{(i)}, \quad (100)$$

where $z_c^{(i)}$ are distributed with the critical distribution $Q_c(z)$.

As in the wetting case, the recurrence of Eq. (101) coincides with the recurrence describing a directed polymer on a Cayley tree [23,24], with the following differences. (i) The variables δ_n are random variables of zero mean [Eq. (98)], which is equivalent to a directed polymer model with random signs studied in Ref. [25]. (ii) More importantly, the random weights $\frac{z_c}{b}$ are distributed with the fixed point distribution $Q_c(z)$ presenting a broad power-law tail in $1/z_c^{1+\mu}$ with $1<\mu<2$ (instead of $0<\mu<1$ for the wetting case).

Reasoning as in the wetting case, any narrow symmetric distribution $\mathcal{P}_0(\delta_0)=\mathcal{P}_0(-\delta_0)$ will lead to power-law tails of index $(1+\mu)$ after one iteration. The study of the evolution of these tails by iteration yields that the corresponding Lyapunov exponent v will be determined by an equation similar to Eq. (49)

$$e^{\mu v} = \frac{2b\overline{z_c^{\mu}}}{\mathcal{B}^{\mu}} + \frac{2b}{\mathcal{B}^{\mu}} \int_0^{+\infty} dy \frac{P_{\infty}(y)}{B_+} y^{\mu} = 1 + \frac{2b}{\mathcal{B}^{\mu}} \int_0^{+\infty} dy \frac{P_{\infty}(y)}{B_+} y^{\mu}, \quad (101)$$

where we have used Eq. (88), in terms of the stationary distribution $P_{\infty}(y)$ of the rescaled process associated to Eq. (100)

$$y_{n+1} = e^{-v} \sum_{i=1}^{2b} \frac{z_c^{(i)}}{\mathcal{B}} y_n^{(i)}. \quad (102)$$

The correlation length exponent then reads $\nu=\frac{\ln 2}{v}$. As in the wetting case, the presence of the second term in Eq. (101) is crucial to obtain a positive v and a finite ν.

V. NUMERICAL STUDY OF THE DIRECTED POLYMER TRANSITION

As for the wetting transition (see Sec. III A), we have used the "pool-method" with a pool number $N=4\times 10^7$ to study the transition of the hierarchical lattice of branching ratio $b=5$ with initial Gaussian energies [Eq. (3)]. The exact bounds on the critical temperature are [14]

$$T_0(b) = \frac{1}{[2 \ln b]^{1/2}} \simeq 0.557 \ldots \leq T_c(b) \leq T_2(b) = \frac{1}{[\ln(b-1)]^{1/2}} \simeq 0.849. \quad (103)$$

In Ref. [14], the phase transition has been studied numerically via the specific heat and the overlap. In this paper, we characterize the transition via the statistics of free energy and energy. As in the wetting case, this allows one to locate very precisely the pool-dependent critical temperature and to measure the divergence of the correlation length $\xi(T)$ above and below T_c.

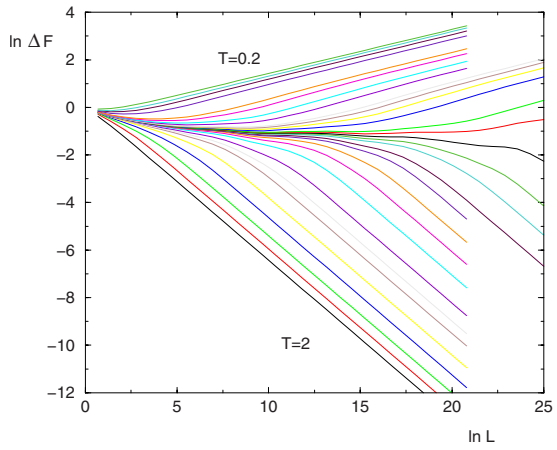

FIG. 6. (Color online) Directed polymer transition: log-log plot of the width $\Delta F(L)$ of the free-energy distribution as a function of L, for many temperatures.

A. Flow of the free-energy width

The flow of the free-energy width ΔF_L as L grows is shown on Fig. 6 for many temperatures. One clearly sees the two attractive fixed points. For $T>T_c$, the free-energy width decays asymptotically with the exponent $\omega_{\infty}(b)$ introduced in Eq. (72)

$$\Delta F(L) \simeq \left(\frac{L}{\xi_F^+(T)} \right)^{-\omega_{\infty}(b)} \quad \text{with} \quad \omega_{\infty}(b=5) = \frac{\ln(b/2)}{2 \ln 2} = 0.6609, \quad (104)$$

where $\xi_F^+(T)$ is the corresponding correlation length that diverges as $T \to T_c^+$.

For $T<T_c$, the free-energy width grows asymptotically with the exponent $\omega_0(b)$ of the ground-state energy distribution

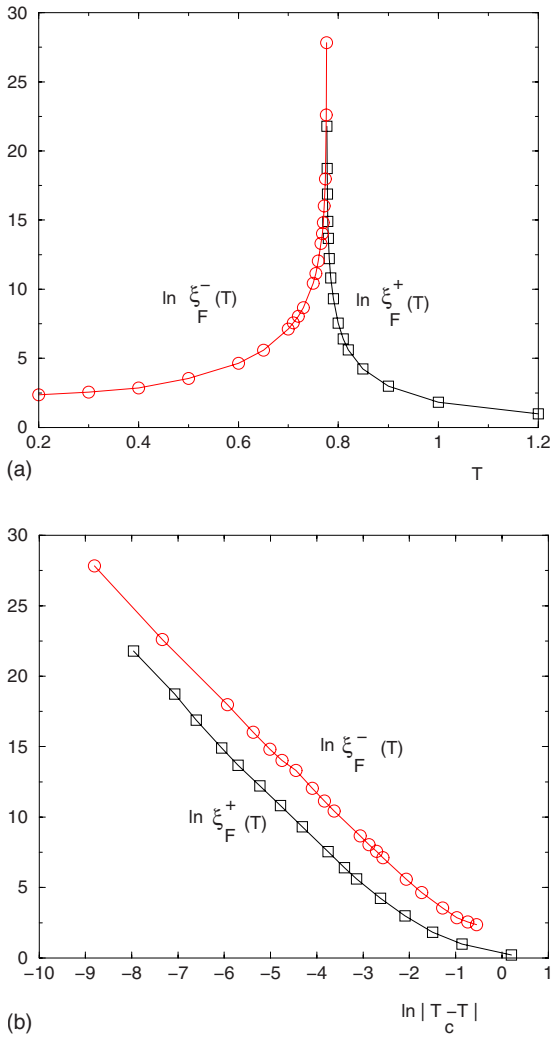

FIG. 7. (Color online) Directed polymer transition: Correlation length $\xi_F^{\pm}(T)$ as measured from the behavior of the free-energy width [Eqs. (104) and (105)]. (a) $\ln \xi_F^{\pm}(T)$ as a function of T. (b) $\ln \xi_F^{\pm}(T)$ as a function of $\ln|T_c - T|$: the asymptotic slopes are of order $\nu \sim 3.4$.

$$\Delta F(L) \simeq \left(\frac{L}{\xi_F^-(T)}\right)^{\omega_0(b)} \quad \text{with} \quad \omega_0(b=5) \simeq 0.186\ldots, \tag{105}$$

where $\xi_F^-(T)$ is the corresponding correlation length that diverges as $T \to T_c^-$. For each given pool, the flow of free-energy width allows a very precise determination of the pool-dependent critical temperature, for instance, in the case considered $0.776\,62 < T_c^{\text{pool}} < 0.776\,66$ which is significantly below the upper bound T_2 of Eq. (103).

B. Divergence of the correlation lengths $\xi_F^{\pm}(T)$

The correlation lengths $\xi_F^{\pm}(T)$ as measured from the free-energy width asymptotic behaviors above and below T_c [Eqs. (104) and (105)] are shown in Fig. 7(a). The plot in terms of the variable $\ln|T_c - T|$ shown in Fig. 7(b) indicate a power-law divergence with the same exponent

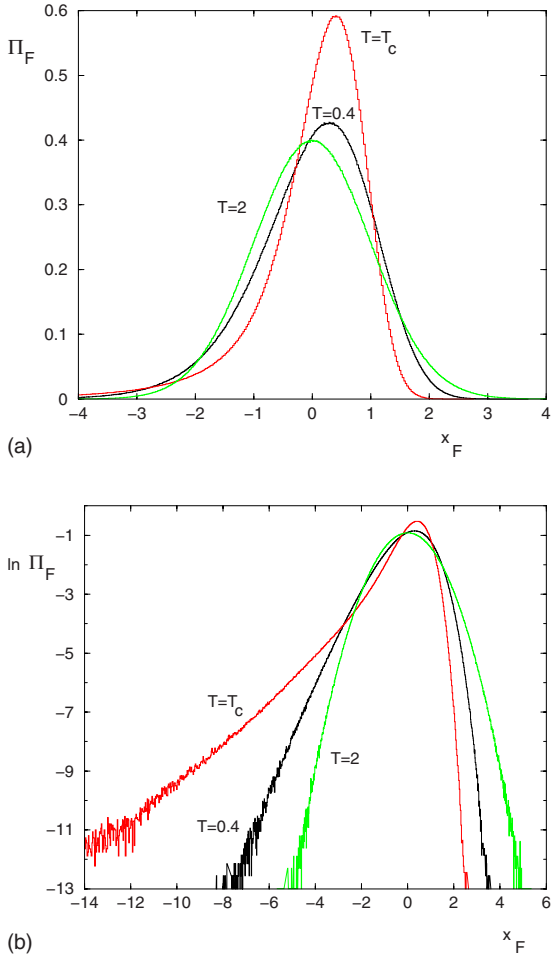

FIG. 8. (Color online) Directed polymer transition: Asymptotic distribution Π_F of the rescaled free-energy $x_F = \frac{F - F_{\text{av}(L)}}{\Delta F(L)}$ in the low-temperature phase (here $T=0.4$), in the high-temperature phase (here $T=2$) and at criticality (here $T_c^{\text{pool}} = 0.776\,65$). (a) Bulk representation. (b) Log representation to see the tails.

$$\xi_F^{\pm}(T) \underset{T \to T_c}{\propto} |T - T_c|^{-\nu} \quad \text{with} \quad \nu \simeq 3.4. \tag{106}$$

C. Histogram of the free-energy

The asymptotic probability distribution Π_F of the rescaled free-energy

$$x_F \equiv \frac{F - F_{\text{av}(L)}}{\Delta F(L)} \tag{107}$$

is shown in Fig. 8 for three temperatures. (i) for $T > T_c$, it is a Gaussian in agreement with Eq. (71). (ii) For $T < T_c$, it coincides with the ground-state energy distribution. (iii) At criticality, one clearly see that a left-tail develops with tail exponent $\eta_c = 1$ in agreement with Eq. (80). The corresponding power-law exponent of Eq. (26) of the fixed-point distribution of Eq. (25) is of order

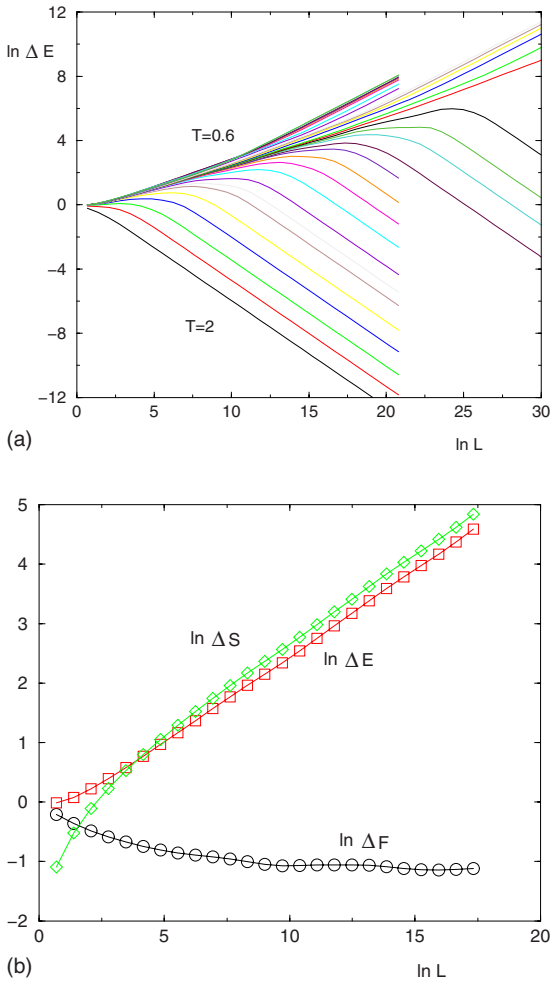

FIG. 9. (Color online) Directed polymer transition: Flow of the widths $\Delta E(L)$ of the energy distribution as L grows. (a) $\ln \Delta E(L)$ as a function of $\ln L$ for many temperatures. (b) Comparison of $\ln \Delta E(L)$, $\ln \Delta S(L)$, and $\ln \Delta F(L)$ as a function of $\ln L$ at criticality ($T_c^{\text{pool}}=0.776\,65$).

$$\mu \sim 1.6. \tag{108}$$

Again this measure is not precise as a consequence of the unknown logarithmic correction in Eq. (25), but it is in the expected interval of Eq. (93).

D. Flow of the energy and entropy widths

The flow of the energy width $\Delta E(L)$ as L grows is shown on Fig. 9(a) for many temperatures [the flow of the entropy width $\Delta S(L)$ is very similar at large scale]. For $T>T_c$, we find that these widths decay asymptotically with the same exponent $\omega_\infty(b)$ as the free energy [Eq. (104)]

$$\Delta E(L) \simeq L^{-\omega_\infty(b)}, \tag{109}$$

$$\Delta S(L) \simeq L^{-\omega_\infty(b)}. \tag{110}$$

For $T<T_c$, in agreement with the Fisher-Huse droplet scaling theory for directed polymers [26], we find that these widths grow asymptotically with the exponent 1/2 which is bigger than the free-energy exponent $\omega_0(b)$ [Eq. (105)]

$$\Delta E(L) \simeq L^{1/2}, \tag{111}$$

$$\Delta S(L) \simeq L^{1/2}. \tag{112}$$

Exactly at criticality, the free-energy $\Delta F(L)$ width converges toward a constant, whereas the energy and entropy widths grow as power laws [see Fig. 9(b)]

$$\Delta E(L) \sim L^{y_c} \sim \Delta S(L) \quad \text{with} \quad y_c \sim 0.29. \tag{113}$$

This exponent is in agreement with the finite-size scaling relation $y_c=1/\nu$ with $\nu \sim 3.4$ [see Eqs. (106)].

E. Divergence of the correlation lengths $\xi_E^{\pm}(T)$, $\xi_S^{\pm}(T)$

According to the Fisher-Huse droplet scaling theory of spin glasses [26], the singularities of the widths of energy and entropy as $T \to T_c^-$ is given by $[L/\xi(T)]^{1/2}/(T_c-T)$. We thus define the correlation lengths $\xi_E^+(T)$ and $\xi_S^+(T)$ by

$$\Delta E(L) \simeq \frac{1}{T_c - T}\left(\frac{L}{\xi_E^-(T)}\right)^{1/2}, \tag{114}$$

$$\Delta S(L) \simeq \frac{1}{T_c - T}\left(\frac{L}{\xi_S^-(T)}\right)^{1/2}. \tag{115}$$

Similarly, for $T>T_c$, we define the corresponding correlation lengths $\xi_E^+(T)$ and $\xi_S^+(T)$ by the equations

$$\Delta E(L) \simeq \frac{1}{T - T_c}\left(\frac{L}{\xi_E^+(T)}\right)^{-\omega_\infty(b)}, \tag{116}$$

$$\Delta S(L) \simeq \frac{1}{T - T_c}\left(\frac{L}{\xi_S^+(T)}\right)^{-\omega_\infty(b)}. \tag{117}$$

The correlations lengths are shown in Fig. 10(a) The plot in terms of the variable $\ln|T_c-T|$ shown in Fig. 10(b) indicate a power-law divergence with the same exponent as in Eq. (106)

$$\xi_E^{\pm}(T) \underset{T \to T_c}{\propto} |T - T_c|^{-\nu} \quad \text{with} \quad \nu \simeq 3.4. \tag{118}$$

F. Histogram of the energy

The asymptotic probability distribution Π_E of the rescaled energy

$$x_E \equiv \frac{E - E_{\text{av}(L)}}{\Delta E(L)} \tag{119}$$

is shown for three temperatures on Fig. 11 (i) outside criticality, both for $T>T_c$ and $T<T_c$, these distributions are Gaussian. (ii) At criticality, the distribution is strongly non-Gaussian and asymmetric, with a left-tail of tail exponent $\eta_c=1$.

VI. COMPARISON WITH CORRESPONDING RESULTS ON HYPERCUBIC LATTICES

Since the exact renormalizations on the diamond lattice can also be considered as approximate Migdal-Kadanoff

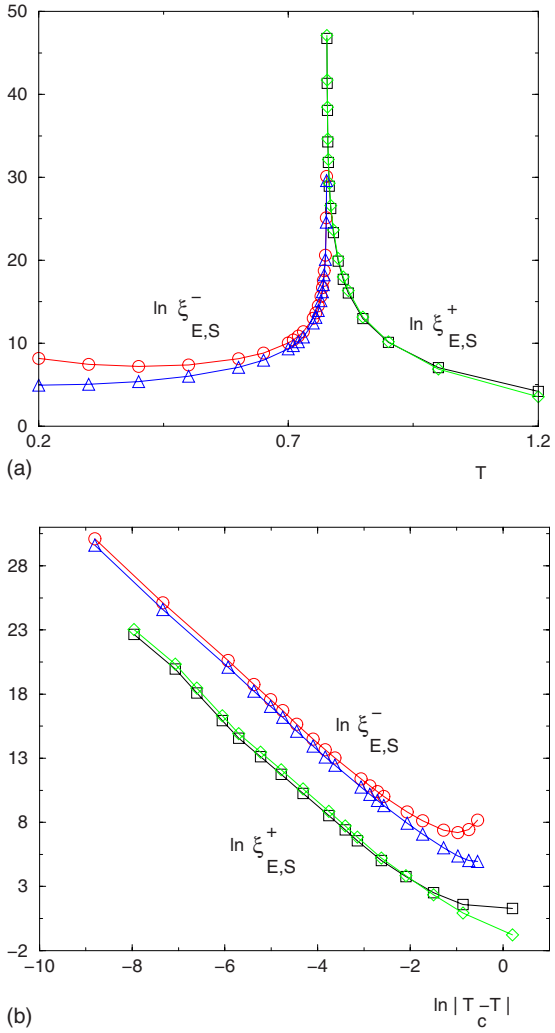

FIG. 10. (Color online) Directed polymer transition: Correlation length $\xi_E^{\pm}(T)$ (circles below and square above) and $\xi_S^{\pm}(T)$ (triangles below and diamond above) as measured from the behavior of the energy and entropy widths. (a) $\ln \xi_E(T)$ and $\ln \xi_S(T)$ as a function of T. (b) $\ln \xi_E(T)$ and $\ln \xi_S(T)$ as a function of $\ln|T_c-T|$: the asymptotic slopes are of order $\nu \sim 3.4$ as in Fig. 7.

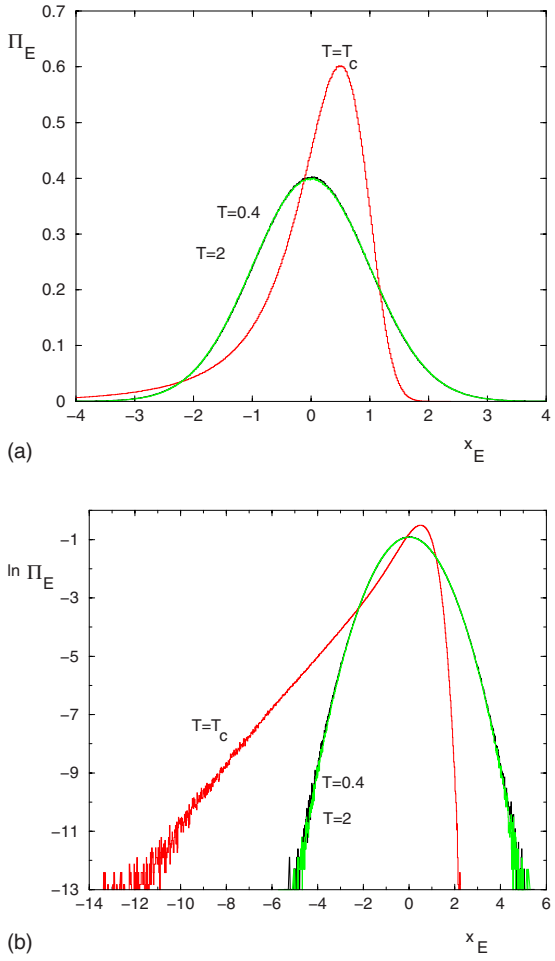

FIG. 11. (Color online) Directed polymer transition: Asymptotic distribution Π_E of the rescaled energy $x=\frac{E-E_{\text{av}}}{\Delta E}$ in the low-temperature phase (here $T=0.4$), in the high-temperature phase (here $T=2$), and at criticality ($T_c^{\text{pool}}=0.776\,65$). (a) Bulk representation. (b) Log-representation to see the tails.

renormalizations for hypercubic lattices, it is interesting to discuss whether the results obtained for the wetting and the directed polymer on the diamond lattice are qualitatively similar to the results for hypercubic lattices.

A. Similarities for $T<T_c$

The whole low-temperature phase of disordered systems is usually characterized by the zero-temperature fixed point where disorder fluctuations dominate. For the disordered polymer models considered in this paper, the free-energy fluctuations grow as a power law of the length both for the diamond lattice and for the hypercubic lattice

$$\Delta F(L,T<T_c) \underset{L\to\infty}{\propto} L^{\omega_0}, \tag{120}$$

where ω_0 is the exponent governing the fluctuations of the ground-state energy $E_0(L)$. In the wetting case, this exponent has the simple value $\omega_0^{\text{wett}}=1/2$ that reflects the normal fluctuations of the L random variables defining the random adsorbing energies along the wall. In the directed polymer case, the exponent ω_0 is nontrivial because the ground-state configuration is the result of an optimization problem.

B. Differences for $T>T_c$

The high-temperature phase of disordered systems is characterized by bounded disorder fluctuations but these fluctuations are not of the same order on diamond lattices and on hypercubic lattices. More precisely, for the disordered polymer models considered in this paper, the free-energy fluctuations decays as a power law on the diamond lattices, whereas they remain of order $O(1)$ on hypercubic lattices

$$\text{diamond:} \quad \Delta F(L,T>T_c) \underset{L\to\infty}{\propto} L^{-\omega_\infty(b)}, \tag{121}$$

$$\text{hypercubic:} \quad \Delta F(L,T>T_c) \underset{L\to\infty}{\propto} O(1). \tag{122}$$

This difference seems to come from the following boundary conditions. (i) On the diamond lattice, the polymer is fixed at

the two extreme points, but by the iterative construction of the lattice, the coordinence of these two extreme points grow with the number n of generations, so that it is possible to have a very efficient averaging even near the boundaries. (ii) On the hypercubic lattices, the boundary conditions are sufficient to produce free-energies fluctuations of order $O(1)$: The fixed origin has a finite coordinence and the fluctuations of order $O(1)$ of the random variables near this origin do not disappear as $L \to \infty$.

C. Differences at criticality

On the hierarchical lattice, the free-energy fluctuations of the disordered polymer considered here are of order $O(1)$ at criticality

$$\text{diamond:} \quad \Delta F(L, T = T_c) \underset{L \to \infty}{\propto} O(1) \tag{123}$$

and it is the only possibility in the presence of exact renormalizations: if the free-energy width is growing, the flow will be attracted at large scale toward the zero-temperature fixed point of Eq. (120), whereas if free-energy width is decaying, the flow will be attracted toward the high-temperature fixed point of Eq. (122). On hypercubic lattices, the free-energy fluctuations $\Delta F(L, T_c) \sim L^{\omega_c}$ at criticality are expected to be governed by a vanishing exponent $\omega_c = 0$, but they are not necessarily of order $O(1)$ because logarithms cannot be excluded, and have actually been found for the directed polymer transition as we now explain. Forrest and Tang [27] have conjectured from their numerical results on a growth model in the KPZ universality class and from the exact solution of another growth model that the fluctuations of the height of the interface were logarithmic at criticality. For the directed polymer model, this translates into a logarithmic behavior of the free energy fluctuations at T_c

$$\text{hypercubic:} \quad \Delta F^{3d}_{\mathrm{DP}}(L, T = T_c) \underset{L \to \infty}{\propto} (\ln L)^{\sigma}, \tag{124}$$

where the exponent was measured to be $\sigma = 1/2$ in $d=3$ [27–29]. Further theoretical arguments in favor of this logarithmic behavior can be found in Refs. [30,31]. So the scaling of free-energy fluctuations at criticality seem to be different on hypercubic lattices and on diamond lattices.

Another related issue concerns the location of the critical temperature T_c with respect to upper bound T_2. (i) On the diamond lattice, the ratio r_2 of Eq. (91) is finite at T_2, the ratio $z = Z/Z_{\mathrm{ann}}$ is a finite random variable at T_c, but the probability distribution of the corresponding partition function presents a power-law tail of index $(1+\mu)$ with $1 < \mu < 2$ [Eq. (93)], leading to the strict inequality $T_c < T_2$. (ii) On hypercubic lattices, the location of T_c with respect to T_2 is still controversial. In Ref. [32], we have argued that $T_c = T_2$ in dimension $d=3$, because the divergence of $r_2 \sim e^{a \ln L}$ at T_2 is compatible with the logarithmic free-energy fluctuations of Eq. (124), provided the rescaled distribution of free-energy involves a left-tail exponent $\eta_c > 1$, as measured numerically in Ref. [29]. In Ref. [33], we have also found clear numerical evidence from the statistics of inverse participation ratios that the delocalization transition takes place at T_2. However, other arguments are in favor of the strict inequality $T_c < T_2$ in finite dimensions: A new upper bound $T^* < T_2$ was proposed in $1+3$ [34] and in Ref. [35] the location of T_c with respect to T_2 was shown to depend upon dimension and probability distribution of the bond energies. In particular for the Gaussian distribution, the result $T_c < T_2$ is obtained only for $d \geq 5$ [35], but not for the case $d=3$ considered in numerical simulations [29,33]. For the wetting transition in $1+1$ dimension, we are not aware of results concerning the scale of free-energy fluctuations at criticality.

This comparison between the diamond lattice and hypercubic lattice can be summarized as follows. The free-energy fluctuations present analogous power-law behaviors in the low-temperature phase [Eq. (120)] but have different behaviors in the high-temperature phase [Eq. (122)]. At criticality, the free-energy fluctuations could also scale differently if logarithmic contributions are present on regular lattices.

VII. CONCLUSION

In this paper, we have studied the wetting transition and the directed polymer delocalization transition on diamond hierarchical lattices. These two phase transitions with frozen disorder correspond to the critical points of quadratic renormalizations of the partition function. We have first explained why the comparison with multiplicative stochastic processes allows one to understand the presence of a power-law tail in the fixed point distribution $P_c(z) \sim \Phi(z)/z^{1+\mu}$ as $z \to +\infty$ [up to some subleading logarithmic function $\Phi(z)$] so that all moments z^n with $n > \mu$ diverge. The exponent μ is in the range $0 < \mu < 1$ for the wetting transition (the first moment diverges $\overline{z} = +\infty$ and the critical temperature is strictly below the annealed temperature $T_c < T_{\mathrm{ann}}$) and is the range $1 < \mu < 2$ for the directed polymer transition (the second moment diverges $\overline{z^2} = +\infty$ and the critical temperature is strictly below the transition temperature T_2 of the second moment). We then obtained that the linearized renormalization around the critical point, which determines the exponent ν, coincides with the transfer matrix describing a directed polymer on the Cayley tree, where the random weights determined by the fixed point distribution $P_c(z)$ are broadly distributed. We have shown that it induces important differences with respect to the usual traveling wave solutions concerning more narrow distributions of the weights [23–25], where the selected velocity only depends on the tail region. Note that traveling waves also appear in other renormalization approaches of random systems [36]. Finally, we have presented detailed numerical results on the statistics of the free-energy and of the energy as a function of temperature for the wetting and the directed polymer transition on the diamond hierarchical lattice with branching ratio $b=5$. In particular, we have shown that the measure of the free-energy width $\Delta F(L)$ yields a very clear signature of the transition and allows one to measure the divergence of the correlation length $\xi^{\pm}(T)$ both below and above T_c: (i) for $T < T_c$, the free-energy width is governed by the zero-temperature exponent ω_0 via $\Delta F(L) \sim [L/\xi_-(T)]^{\omega_0}$; (ii) for $T > T_c$, the free-energy width is governed by the high-temperature exponent ω_∞ via $\Delta F(L) \sim [L/\xi_+(T)]^{-\omega_\infty}$. From the point of view of histograms, the

development of a left tail with exponent $\eta_c=1$ at criticality is very clear and different from histograms with exponent $\eta>1$ outside criticality.

APPENDIX: REMINDER ON MULTIPLICATIVE STOCHASTIC PROCESSES

Multiplicative stochastic processes appears in many contexts, in particular in one-dimensional disordered systems, such as random walk in random potentials [37–39] or random spin chains [40,41] In this Appendix, we recall some useful results concerning the following recurrence of random variables X_n:

$$X_{n+1} = a_n X_n + b_n, \tag{A1}$$

where (a_n, b_n) are positive independent random numbers. The condition to have a stationary probability distribution $P_\infty(X)$ is

$$\overline{\ln a} < 0. \tag{A2}$$

The most important property of $P_\infty(X)$ is that it presents a power-law tail

$$P_\infty(X) \underset{X\to+\infty}{\simeq} \frac{C}{X^{1+\mu}}, \tag{A3}$$

where the exponent $\mu>0$ is determined by the condition [37–41]

$$\overline{a^\mu} = 1. \tag{A4}$$

To understand where this condition comes from, one needs to write that $P_\infty(X)$ is stable via the iteration of Eq. (A1)

$$P_\infty(X) = \int da\mathcal{P}(a)\int db\psi(b)\int dY P_\infty(Y)\delta[X-(aY+b)]$$

$$= \int da\mathcal{P}(a)\int db\psi(b)\frac{P_\infty\left(\frac{X-b}{a}\right)}{a}, \tag{A5}$$

where $\mathcal{P}(a)$ and $\psi(b)$ are the probability distributions of a_n and b_n, respectively. The stability of the power-law tail of Eq. (A3) in the region $X\to+\infty$ yields at leading order

$$\frac{C}{X^{1+\mu}} \simeq \int da\mathcal{P}(a)\int db\psi(b)a^\mu\frac{C}{X^{1+\mu}} = \overline{a^\mu}\frac{C}{X^{1+\mu}} \tag{A6}$$

yielding the condition of Eq. (A4).

[1] Th. Niemeijer and J. M. J. van Leeuwen, in *Phase Transitions and Critical Phenomena*, edited by C. Domb and M. S. Green (Academic, New York, 1976); in *Real Space Renormalization*, edited by T. W. Burkhardt and J. M. J. van Leeuwen, Topics in Current Physics Vol. 30 (Springer, Berlin, 1982); B. Hu, Phys. Rep. **91**, 233 (1982).
[2] F. Igloi and C. Monthus, Phys. Rep. **412**, 277 (2005).
[3] S.-K. Ma, C. Dasgupta, and C.-k. Hu, Phys. Rev. Lett. **43**, 1434 (1979); C. Dasgupta and S.-K. Ma, Phys. Rev. B **22**, 1305 (1980).
[4] D. S. Fisher, Phys. Rev. Lett. **69**, 534 (1992); Phys. Rev. B **50**, 3799 (1994); **51**, 6411 (1995).
[5] A. A. Migdal, Sov. Phys. JETP **42**, 743 (1976); L. P. Kadanoff, Ann. Phys. **100**, 359 (1976).
[6] A. N. Berker and S. Ostlund, J. Phys. C **12**, 4961 (1979).
[7] M. Kaufman and R. B. Griffiths, Phys. Rev. B **24**, 496 (1981); R. B. Griffiths and M. Kaufman, *ibid.* **26**, 5022 (1982); M. Kaufman and R. B. Griffiths, *ibid.* **30**, 244 (1984).
[8] C. Jayaprakash, E. K. Riedel, and M. Wortis, Phys. Rev. B **18**, 2244 (1978).
[9] W. Kinzel and E. Domany, Phys. Rev. B **23**, 3421 (1981); B. Derrida and E. Gardner, J. Phys. A **17**, 3223 (1984); D. Andelman and A. N. Berker, Phys. Rev. B **29**, 2630 (1984).
[10] See, for instance, A. P. Young and R. B. Stinchcombe, J. Phys. C **9**, 4419 (1976); B. W. Southern and A. P. Young, *ibid.* **10**, 2179 (1977); S. R. McKay, A. N. Berker, and S. Kirkpatrick, Phys. Rev. Lett. **48**, 767 (1982); A. J. Bray and M. A. Moore, J. Phys. C **17**, L463 (1984); E. Gardner, J. Phys. (France) **45**, 115 (1984); M. Nifle and H. J. Hilhorst, Phys. Rev. Lett. **68**, 2992 (1992); M. Ney-Nifle and H. J. Hilhorst, Physica A **194**, 462 (1993); M. A. Moore, H. Bokil, and B. Drossel, Phys. Rev. Lett. **81**, 4252 (1998).
[11] B. Derrida, V. Hakim, and J. Vannimenus, J. Stat. Phys. **66**, 1189 (1992).
[12] L. H. Tang and H. Chaté, Phys. Rev. Lett. **86**, 830 (2001).
[13] B. Derrida and R. B. Griffiths, Europhys. Lett. **8**, 111 (1989).
[14] J. Cook and B. Derrida, J. Stat. Phys. **57**, 89 (1989).
[15] T. Halpin-Healy, Phys. Rev. Lett. **63**, 917 (1989); Phys. Rev. A **42**, 711 (1990).
[16] S. Roux, A. Hansen, L. R. da Silva, L. S. Lucena, and R. B. Pandey, J. Stat. Phys. **65**, 183 (1991).
[17] L. Balents and M. Kardar, J. Stat. Phys. **67**, 1 (1992); E. Medina and M. Kardar, *ibid.* **71**, 967 (1993).
[18] M. S. Cao, J. Stat. Phys. **71**, 51 (1993).
[19] L. H. Tang, J. Stat. Phys. **77**, 581 (1994).
[20] S. Mukherji and S. M. Bhattacharjee, Phys. Rev. E **52**, 1930 (1995).
[21] R. A. da Silveira and J. P. Bouchaud, Phys. Rev. Lett. **93**, 015901 (2004).
[22] T. Halpin-Healy and Y.-C. Zhang, Phys. Rep. **254**, 215 (1995).
[23] B. Derrida and H. Spohn, J. Stat. Phys. **51**, 817 (1988).
[24] B. Derrida, Phys. Scr. **38**, 6 (1991).
[25] J. Cook and B. Derrida, J. Stat. Phys. **61**, 961 (1990); B. Derrida, M. R. Evans, and E. R. Speer, Commun. Math. Phys. **156**, 221 (1993).
[26] D. S. Fisher and D. A. Huse, Phys. Rev. B **43**, 10728 (1991).
[27] B. M. Forrest and L.-H. Tang, Phys. Rev. Lett. **64**, 1405 (1990).
[28] J. M. Kim, A. J. Bray, and M. A. Moore, Phys. Rev. A **44**, R4782 (1991).
[29] C. Monthus and T. Garel, Eur. Phys. J. B **53**, 39 (2006).
[30] L.-H. Tang, T. Nattermann, and B. M. Forrest, Phys. Rev. Lett. **65**, 2422 (1990).
[31] C. A. Doty and J. M. Kosterlitz, Phys. Rev. Lett. **69**, 1979

(1992).
[32] C. Monthus and T. Garel, Phys. Rev. E **74**, 011101 (2006).
[33] C. Monthus and T. Garel, Phys. Rev. E **75**, 051122 (2007).
[34] M. Birkner, Electron. Commun. Probab. **9**, 22 (2004); M. Birkner, Ph.D. thesis, J.W. Goethe Universität, Frankfurt, 2003, http://publikationen.ub.uni-frankfurt.de/volltexte/2003/314/
[35] A. Camanes and P. Carmona, http://www.math.sciences.univ-nantes.fr/camanes/recherche.html.
[36] D. Carpentier and P. Le Doussal, Phys. Rev. Lett. **81**, 2558 (1998); Nucl. Phys. B **588**, 565 (2000); Phys. Rev. E **63**, 026110 (2001).
[37] H. Kesten, Acta Math. **131**, 207 (1973); H. Kesten *et al.*, Compos. Math. **30**, 145 (1975).
[38] B. Derrida and Y. Pomeau, Phys. Rev. Lett. **48**, 627 (1982).
[39] J. P. Bouchaud and A. Georges, Phys. Rep. **195**, 127 (1990).
[40] B. Derrida and H. Hilhorst, J. Phys. A **16**, 2641 (1983).
[41] C. de Callan, J. M. Luck, Th. Nieuwenhuizen, and D. Petritis, J. Phys. A **18**, 501 (1985).